Water Resources Management
https://doi.org/10.1007/s11269-025-04162-1

Projecting Depth-Duration-Frequency Curves for Future Climate: a Case Study in the Mediterranean Area

Dario Treppiedi[1] · **Antonio Francipane**[1] · **Leonardo Valerio Noto**[1]

Received: 27 November 2024 / Accepted: 24 February 2025

Abstract

Depth-Duration-Frequency (DDF) curves are an essential tool in hydrological planning and risk management. However, the assumption of stationarity that is traditionally embedded in their derivation, is increasingly questioned by the impacts of climate change. This study focuses on adapting and projecting DDF curves for Sicily (Italy), which is experiencing an intensification of rainfall extremes, particularly for shorter durations. The proposed framework adapts the most up-to-date regional frequency analysis for the island by using an adaptation factor that incorporates the thermodynamic relationship between extreme precipitation and temperature, as well as future climate projections for temperature from an ensemble of regional climate models under the worst-case scenario. By the end of the century, the design rainfall estimates may require to be increased up to 50%, especially for hourly durations, to account for climate change effects. The results also highlight a strong spatial variability in the precipitation quantiles, with higher values observed in specific areas such as the north-eastern part of the island, which is characterized by small catchments and particularly prone to flash floods. Finally, this study provides a simple but still physical-based approach to updating DDF curves, that can be useful for engineers and practitioners, enhancing international efforts to mitigate climate change impacts through improved hydrological planning.

Highlights

- Future DDF curves for Sicily are provided through a quasi-stationary framework
- Combining CC-scaling and temperature projections shows an increase up to 50% for design rainfall
- Hourly durations may exhibit the most significant changes in the future
- The methodology aligns with revising DDF frameworks in a climate change context

Keywords DDF; IDF · Climate change · Scaling coefficient · RCM projections

✉ Leonardo Valerio Noto
leonardo.noto@unipa.it

[1] Dipartimento di Ingegneria, Università degli Studi di Palermo, Palermo, Italy

Published online: 12 March 2025

1 Introduction

Depth-Duration-Frequency (DDF, or Intensity-Duration-Frequency, IDF) curves have always been an essential tool for engineers, practitioners, and researchers who deal with hydrology and water resource management. By describing the relationship between the depth (or intensity), duration, and frequency (often referred to as return period) of intense rainfall, these curves make it possible to infer the probability that an event, characterized by a certain duration and magnitude, may occur in a given period of time. From this definition, it is trivial to recognize their central role in the design of drainage systems (Brown et al. 2001) or water management infrastructures, such as dams, dikes, spillways, and hydraulic infrastructures in general (Shehu et al. 2023). They are also a key component in flood risk management, helping to model flood hazard and quantify rainfall-driven flooding scenarios.

Traditionally, data availability has been regarded as crucial for the accuracy of DDF curves, given the statistical framework underlying their formulation. More recently, however, researchers have turned their attention to the fact that stationarity assumption has long been compromised by the effects of human activities, leading to the need to develop non-stationary frameworks and models to optimize water systems and manage water resources in the future (Milly et al. 2008; Tsakiris and Loucks 2023). Extreme rainfall events are becoming more intense and frequent in different areas of the world (Masson-Delmotte et al. 2021; Treppiedi et al. 2025), and anthropogenic role in this change has been widely demonstrated (Fowler et al. 2021). These alterations are influenced by shifts in both atmospheric dynamics and thermodynamic processes (O'Gorman 2015; Pfahl et al. 2017). In this context, the Clausius-Clapeyron (CC) relationship has been largely used to explain the thermodynamic contribution to this change (Lenderink et al. 2017; Fischer and Knutti 2016). According to this relationship the atmosphere's capacity to hold water vapor increases by approximately 7% for every 1 °C rise in temperature. This suggests that warmer conditions lead to a higher probability of having a water content sufficient to fuel more intense precipitation events, when the right atmospheric conditions are also present.

Given the evidence that climate change is altering the characteristics of extreme events, how reliable can DDF estimates remain if they assume that these phenomena are not changing? Hence, several methods have been developed to integrate non-stationarity in the DDF framework.

According to Schlef et al. (2023), these techniques can be summarized into three main categories:

- ***Extreme value distribution (EVD) fitting in quasi-stationary time periods***. This method involves fitting an EVD to precipitation extremes at different durations within quasi-stationary time periods. It is widely used to detect changes in DDF by considering future scenarios from global and regional climate models (GCMs and RCM, respectively) (Noor et al. 2022; Zhao et al. 2021) or from convection-permitting models (CPMs) (Dallan et al. 2024). However, some limitations may arise when only time-limited sets of observations are available, which can make model validation challenging and increase the difficulty of robustly estimating changes in higher statistical moments (Salas et al. 2018).
- ***Non-stationary EVD with covariates***. In this approach, one or more parameters of the EVD depend on covariates, which can explain the causative mechanism affecting the

extreme precipitation. The most used covariate is time (Cheng and AghaKouchak 2014; Sarhadi and Soulis 2017), despite it is not always the most appropriate choice (Agilan and Umamahesh 2017). Other tested covariates for non-stationary analysis include local temperature changes (Mondal and Mujumdar 2015), climate variability indices (Sarhadi and Soulis 2017; Ouarda et al. 2019), and urbanization (Agilan and Umamahesh 2016). In this case, in addition to the difficulties introduced in the previous point, a further limitation may be due to the correct choice of drivers to be considered as covariates, which may vary significantly depending on the study area (Yan et al. 2021).

– ***Scaling approach***. The last approach, briefly mentioned by Schlef et al. (2023), is the scaling approach. This method applies a percentage increase to existing DDF curves based on projected warming, using relationships such as the CC equation. The framework has been thoroughly examined by Martel et al. (2021), who highlighted the challenges associated with its initial formulations and proposed a new approach. Applying the procedure to precipitation and temperature projections from an ensemble of 26 GCMs at the global scale, the authors provide a detailed description of all the terms that need to be estimated, also offering recommendations for practitioners and researchers.

This last methodology offers several advantages; one of these is that DDF curves do not need to be recomputed from scratch, but existing products can be adapted. This feature is particularly useful in those cases where measurement station networks are dismissed, relocated, or replaced, leading to inconsistencies in the data and making it impossible to rely on long series. A second advantage comes from the fact that many regions of the world are not yet covered by CPM ensembles. In this case, this methodology can be particularly beneficial for estimating design rainfall for shorter durations which are driven by convective phenomena, poorly represented in RCMs or GCMs where convection is not explicitly resolved but rather parameterized. Finally, its simplicity helps to bridge the gap between research and practitioners.

The methodology proposed and applied by Martel et al. (2021) at the global scale is particularly valuable for adapting DDF curves also at smaller scales (e.g., regional) when a considerable amount of ground-based data is available. For these reasons, we decided to apply it to the specific context of Sicily island (Italy), for which DDF curves were recently developed through a Regional Frequency Analysis (RFA) using a dataset that spans a significant portion of the 20th century (Forestieri et al. 2018). Over time, this dataset has experienced a reduction in the number of available stations and data. Concurrently, another measurement network began collecting data on key meteorological variables in the early 2000s, offering high temporal resolutions (i.e., sub-hourly) and ensuring excellent temporal continuity.

Several studies conducted on Sicily have shown an increase in the magnitude of extreme precipitation events over time, particularly affecting hourly and sub-hourly rainfall intensities (Arnone et al. 2013; Treppiedi et al. 2021). Moreover, Treppiedi et al. (2023a) questioned the stationary assumption of the DDF curves commonly used in Sicily, demonstrating a remarkable underestimation of rainfall quantiles, especially at shorter durations and lower return periods. These findings require that projected DDF curves account for these changes, in order to more accurately model the future hydrological response of basins, water resources, and hydraulic infrastructure management. Furthermore, Sicily's geographic location also requires special attention regarding temperature variations, since the Mediterranean region is warming faster than many other areas of the world, to the point

of being identified as a climatic hotspot (Giorgi 2006; Zittis et al. 2022). Finally, this should be viewed in an international context that emphasizes the need for updating DDF curves (CSA 2012; Ball et al. 2016), highlighting the pivotal role of research in addressing the challenges posed by climate change (EU 2024).

The paper is organized as follows: Section 2 provides an overview of the study area and a description of the methodology applied. Section 3 presents and discusses the results obtained, while Section 4 contains concluding remarks, highlighting the strengths and limitations of the procedure.

2 Methodology

2.1 Study Area

We focus on Sicily, which is the largest island in the Mediterranean Sea and lies in its center (Fig. 1). Due to its position, the island is characterized by a hot-summer Mediterranean climate (Beck et al. 2018), which is representative of a large portion of the Mediterranean area. Moreover, it represents a transition between the arid climate of North Africa and the temperate climate of Europe. The extent of the island, covering approximately 25,700 km^2, implies that the precipitation regime fluctuates considerably across the territory. The south-

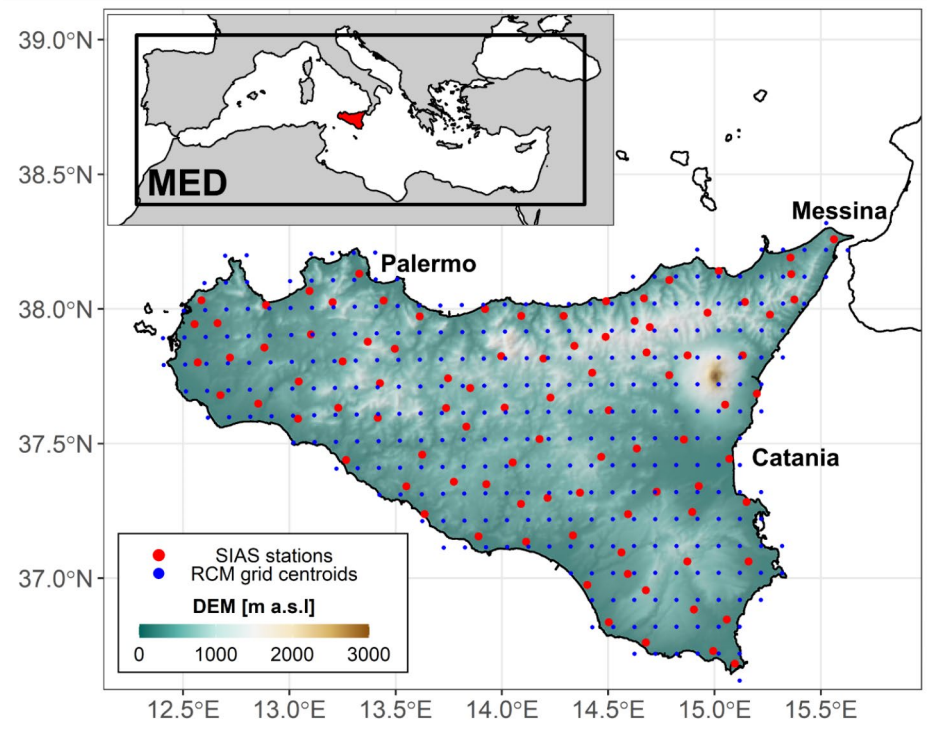

Fig. 1 Spatial distribution of SIAS rain gauges (red dots), overlaid to the digital elevation model (DEM), for Sicily. The blue dots represent the RCM ensemble grid centroids. The upper panel shows the location of the island within the Mediterranean IPCC WGI reference region (Iturbide et al. 2020)

east area is characterized by a mean annual precipitation (MAP) of about 360 mm, while this value is more than five times higher in the northern area, where the contribution of convective precipitation events is particularly relevant (Treppiedi et al. 2023b; Sottile et al. 2022). Concerning temporal variability, winter is generally wetter than summer, despite severe storms may also occur in this season.

2.2 Depth-Duration-Frequency Curves in the Future Climate

To project the DDF in the future climate, the approach proposed by Martel et al. (2021) has been used as a basis for the development of a method specifically based on at site climatic data. According to Martel et al. (2021), the rainfall quantiles of duration *d* and return period *T* for a future scenario ($h_{fut,d,T}$) can be derived as follows:

$$h_{fut,d,RP} = h_{ref,d,RP} \cdot F_{RP} \cdot F_d \cdot \left(\frac{100 + R_{sc,24,2}}{100} \right)^{\Delta T} \tag{1}$$

where $h_{ref,d,RP}$ is the rainfall quantile of duration *d* and return period *RP* for a reference period, $R_{sc,24,2}$ is the CC-scaling of the 24-hour and 2-year return period rainfall in %/°C, F_{RP} and F_d are adjustment factors for all return periods higher than 2 years and durations shorter than 24 h, respectively, and ΔT is the projected change in the seasonal mean temperature expressed in °C.

As stated in the Introduction, the authors apply this framework at the global scale by using an ensemble of GCMs to compute the terms $R_{sc,24,2}$ and ΔT worldwide. However, using GCMs might not be appropriate to more detailed spatial scales, such as in the case of Sicily. These models are developed and generally used for large-scale applications (i.e., the global or macro-regional scale). Indeed, their coarse spatial resolution (e.g., ~1° or more) might result in considering only a few pixels when considering Sicily (e.g., three or four pixels, including both land and sea), not giving spatial distributed information. Also, the parameterization of convection might lead to an underestimation of heavy precipitation events (Mazoyer et al. 2023), which are a relevant contribution in the Mediterranean area especially during summer (Llasat et al. 2021; Treppiedi et al. 2023b). Consequently, using precipitation climate projections from RCMs or GCMs for computing the CC-scaling would result in large underestimates and/or high uncertainties. Moreover only a single-member CPM currently covers the area under examination (Raffa et al. 2023).

Another potential source of uncertainty regards the two adjustment factors F_T and F_d since, as stated by the authors themselves, there is no scientific evidence to retrieve their optimal values. In addition, the need of F_d is to rescale $R_{sc,24,2}$ with duration, since the GCMs employed have daily temporal resolution. This would imply to know how the CC-scaling varies as duration decreases, which is not trivial given the high spatial variability of this coefficient (Ali et al. 2021b).

For all these reasons, we proposed the following formulation to derive the future rainfall quantiles ($h_{fut,d,RP}$):

$$h_{fut,d,RP} = h_{ref,d,RP} \cdot \left(\frac{100 + CC_{obs,d,p^{th}}}{100} \right)^{\bar{\Delta T}_{50}} = h_{ref,d,RP} \cdot F_A \tag{2}$$

where $CC_{obs,d,p^{th}}$ is the CC-scaling at different durations and percentiles that can be derived from an observational dataset, while $\Delta \bar{T}_{50}$ is the projected change in the annual temperature, since DDFs are generally estimated using data from the entire year. We refer to F_A as the 'adaptation factor', representing the multiplicative term for adaptation and projection of DDFs in future climate. The estimation of F_A for Sicily, as well as the data used here, is presented in the next sections.

2.2.1 Reference Rainfall Quantiles ($h_{ref,d,T}$)

Reference rainfall quantiles ($h_{ref,d,RP}$) are a key element to apply Eq. (2), representing what needs to be updated to consider the potential effects of climate change in the future. We use the RFA by Forestieri et al. (2018), which allows defining the reference rainfall quantile for a certain duration (i.e., $1h \leq d \leq 24h$) and return period (i.e., $RP \geq 2\,y$) anywhere in Sicily by using the following equation:

$$h_{ref,d,RP} = K_{RP} \cdot a_{24} \cdot \left(\frac{d}{24}\right)^n \tag{3}$$

where K_{RP} is the regional growth curve for a given return period, evaluated through the two-component extreme value (TCEV) distribution for six homogeneous areas, while a_{24} and n are site-specific parameters, retrieved by means of a linear regression with MAP. Further details can be found in Forestieri et al. (2018).

We used this regional approach as a starting point for several reasons. First, it serves as an effective tool for practitioners, providing spatially distributed estimates of the design rainfall. Also, the regionalization by Forestieri et al. (2018) contains the 'historical' memory of the extreme rainfall regime for the island, since it has been obtained by using the annual maxima from the old Sicilian record networks (i.e., *Autorità di Bacino del Distretto Idrografico della Sicilia*, hereinafter AdB) for the period 1928–2010. In addition, a potential underestimation of design rainfall was recently found by Treppiedi et al. (2023a), who compared the rainfall quantiles obtained with this regional product with those obtained from the newest rain gauge network managed by the *Servizio Informativo Agrometeorologico Siciliano* (hereinafter SIAS - see Section 2.2.2), which covers the period 2002–2023.

2.2.2 Clausius-Clapeyron Scaling Coefficient ($CC_{obs,d,p^{th}}$)

The CC-scaling coefficient ($CC_{obs,d,p^{th}}$ in Eq. 2) represents the thermodynamic factor by which $h_{ref,d,T}$ can be rescaled with changes in temperature (i.e., $\Delta \bar{T}_{50}$). Given the several issues introduced in Section 2.2 in using GCMs or RCMs to compute this coefficient, we derived the CC-scaling from an observational dataset, namely the SIAS network. In particular, we selected all those measurement stations with at least 15 complete years (i.e., more than 85% of data in a year) of hourly precipitation (P), maximum temperature (T_{max}), and maximum relative humidity (RH_{max}) data in the period 2002–2023. We found a total of 92 measuring stations, evenly distributed throughout Sicily (Fig. 1). The dew point temperature (T_{dew}) was then calculated for each of these stations by combining T_{max} and RH_{max} (Magnus 1844).

The procedure to compute the CC-scaling coefficients is summarized as follows:

- we firstly identified the rainy days (RD) as those days when the cumulative precipitation exceeds 1 mm;
- we computed the maximum precipitation ($P_{max,d}$) at different durations (1, 3, 6, and 12 h); the 24-hour duration was disregarded, as it coincides with the time resolution of the previously defined rainy days, increasing the possibility to underestimate the actual cumulative rainfall;
- we associated the T_{dew} at the beginning of each $P_{max,d}$ to observe whether the concurrence of high temperatures and relative humidity can explain the occurrence of intense rainfall events;
- we performed quantile regression (Koenker and Hallock 2001) on $(T_{dew,d},\ log_{10}(P_{max,d}))$ pairs. We selected a very high quantile (i.e., 0.99) to examine how the most intense rainfall events may intensify with temperature. The slopes of the quantile regression lines (i.e., $\gamma_{0.99}$) are then expressed in the typical form of the CC-scaling coefficient (%/°C) following Ali et al. (2022):

$$CC_{obs,d,0.99} = 100 \cdot (10^{\gamma_{0.99}} - 1) \tag{4}$$

At this point, the $CC_{obs,d,0.99}$ values are available for gauged sites within the domain and for some durations. To use these values for adapting and extending the design rainfall from the RFA into the future, it is necessary to have layers that are both continuous for durations and spatially distributed. To solve the first issue, we interpolated the $CC_{obs,d,0.99}$ at each station using a negative power law, deriving the relationship that explains how the coefficient varies within 1 and 24 h:

$$CC_{obs,d,0.99} = \alpha \cdot d^{-\beta} \quad for\ d \in [1, 24] \tag{5}$$

To meet the second requirement, the power-law parameters (i.e., α and β in Eq. 5) were spatially interpolated using Ordinary Kriging (OK), employing the same grid provided by the RCMs (i.e., about 10 km, see Fig. 1); a similar grid size can be also derived also following (Hengl 2006) as a function of study area and rain gauge density.

2.2.3 Projected Changes in the Annual Temperatures ($\Delta\overline{T}_{50}$)

To examine the projected changes in temperature for Sicily region, we considered all the RCMs available at a spatial resolution of ~0.1° in the EURO-CORDEX project (Jacob et al. 2014).We worked with daily temperature data from 16 different RCMs (Table S.1) for the historical experiment (1950–2005) and for the Representative Concentration Pathways (RCP) 8.5 (2006–2100). We decided to use this scenario since it aligns closely with the current emission trajectories (Schwalm et al. 2020), although the framework can be easily extended to other scenarios (e.g., RCP-4.5). Since the RCMs cover the entire European area and have slight different grids, we used the Climate Data Operator from the Max-Planck-Institute for Meteorology (Schulzweida et al. 2019) to crop and interpolate the daily data to a common grid (~10 km, Fig. 1).

At the pixel scale, we calculated the annual average temperature ($\overline{T}$) for each model. To reduce systematic biases, we then created an ensemble of RCM (Moradian et al. 2023).

Specifically, for each year in both the historical and RCPs experiments, we considered the median value of $\bar{T}$ across all the RCMs considered ($\bar{T}_{50}$). In order to compute the $\Delta\bar{T}_{50}$, we split the whole period (i.e., 1950–2100) into five different sub-periods, namely 'Control' (1950–2001), 'Now' (2002–2022), 'Near' (2023–2050), 'Mid' (2051–2075), and 'Far' (2076–2100), aiming to introduce non-stationarity in the DDF framework through a quasi-stationary approach.

Hence, the $\Delta\bar{T}_{50}$ has been computed as follows:

$$\Delta\bar{T}_{50} = \overline{\bar{T}_{50,Period}} - \overline{\bar{T}_{50,Control}} \tag{6}$$

where $\overline{\bar{T}_{50,Control}}$ is the average $\bar{T}_{50}$ in the 'Control' period, while $\overline{\bar{T}_{50,\,Period}}$ is the average $\bar{T}_{50}$ in the 'Now', 'Near, 'Mid and 'Far' periods.

3 Results and Discussion

In this section we show how the $CC_{obs,d,0.99}$ varies spatially across the region, and temporally for different durations, (Section 3.1), and the projected changes in the $\Delta\bar{T}_{50}$ for the four defined periods under the RCP-8.5 (Section 3.2). By combining these two terms with the RFA from Forestieri et al. (2018), we finally provide the adapted and projected DDFs for the 21st century in Sicily (Section 3.3).

3.1 Time Scale and Spatial Dependence of the $CC_{obs,d,0.99}$

Following the procedure described in Section 2.2.2, we derived the $CC_{obs,d,0.99}$ by applying the quantile regression for the 0.99 quantile on the $(T_{dew,d},\ log_{10}(P_{max,d}))$ pairs. This procedure has been applied for each of the 92 measurement stations and for 1-, 3-, 6-, and 12-hour durations. As an example, Figure S.1 shows the empirical $(T_{dew,d},\ log_{10}(P_{max,d}))$ points with the 99th quantile lines for 'Patti' station at the considered durations. We notice that the slope of the quantile line decreases as the duration increases, as confirmed by several other studies (Wasko et al. 2015; Wasko and Sharma 2015). Indeed, for long-duration rainfall events, the moisture advected by large-scale atmospheric dynamics may be more relevant than local changes in air temperature and humidity (Panthou et al. 2014). On the other hand, extreme precipitation events of short duration are mainly sustained by convection, which is related to atmospheric instability driven by high temperatures and humidity (Lenderink and Van Meijgaard 2010). The differences in the slopes with duration may also motivated by the fact that the probability to include dry periods in the cumulative precipitation increases for longer durations (Hardwick Jones et al. 2010). However, we believe that this last aspect is marginal in our analysis, since we defined $P_{max,d}$ starting from rainy days (see Section 2.2.2).

These outcomes are supported by the box plots in Fig. 2a, which show the $CC_{obs,d,0.99}$ (computed using Eq. 4) for all stations at 1-, 3-, 6-, and 12-hour durations. By focusing on the medians, the value for the 1-hour duration hovers around 10%/°C, significantly exceed-

ing the standard 7%/°C. This is similar to what has been observed in other parts of Europe (Lenderink and van Meijgaard 2008; Purr et al. 2021) and worldwide (Ali et al. 2021a; Wasko et al. 2015). Notably, the upper quartile of this distribution approaches 12%/°C, nearing the super CC-scaling (i.e., 14%/°C) (Lenderink et al. 2017). As the duration increases, the median value decreases to approximately 8, 7, and 5%/°C for durations of 3, 6, and 12 h, respectively. The interquartile variability remains almost the same, except for the 12-hour duration where it is possible to observe a slight increase. Additionally, for this latter duration, the lower whisker reaches values close to 0%/°C but remains predominantly positive (with only one negative case). Although not employed in this study, we also computed the $CC_{obs,d,0.99}$ for 10- and 30-min durations (Figure S.2), showing that this trend is also confirmed when passing to sub-hourly durations, albeit with higher variability.

The decrease in $CC_{obs,d,0.99}$ with event duration is modeled using a power-law with negative exponent. Panels b_1) to b_4) in Fig. 2 illustrate, as examples, the curves obtained for four measurement stations. The negative power-law fits the empirical $CC_{obs,d,0.99}$ well, enabling accurate modeling not only in cases where the variation in $CC_{obs,d,0.99}$ with duration is moderate (Fig. 2-b_3), but also in cases with a sharp decay, especially for shorter durations (Fig. 2-b_4). These curves allow for the continuous modeling of $CC_{obs,d,0.99}$ values across all durations between 1 and 24 h, which is essential to integrate this methodology within the RFA framework.

To fully incorporate this methodology, it is also required for the $CC_{obs,d,0.99}$ to be spatially distributed. Panels c_1 and c_2 in Fig. 2 show the interpolated power-law parameters (i.e., α and β, respectively) using the OK interpolation method, together with the at-site empirical values (i.e., dots). For parameter α, which corresponds with the $CC_{obs,d,0.99}$ for 1-h duration, spatial patterns exhibiting values close to the super CC-scaling can be identified in the central-eastern and north-eastern parts of the island. The latter has already been screened as an area particularly interested in convective phenomena, due to the orographic uplift of warm, moisture-laden air masses coming from North Africa (Treppiedi et al. 2023b). Focusing on β parameter, which indicates how rapidly the $CC_{obs,d,0.99}$ decreases with increasing duration, it can be observed that the highest values are concentrated in the Nebrodi Mountains (north) and the southern part of the island. For the sake of completeness, the $CC_{obs,d,0.99}$ maps for 1- to 24-hour durations are shown in Figure S.3.

3.2 Future Projections in Temperature Changes ($\Delta\bar{T}_{50}$)

As stated in Section 2.2, the $\Delta\bar{T}_{50}$ represents the factor accounting for how the $CC_{obs,d,0.99}$ and, in turn, the DDF curves change under the pressure induced by global warming. Figure 3-a depicts the yearly variation in the annual mean temperature ($\bar{T}$) over the period 1950–2100 considering the entire island. We show the evolution of $\bar{T}$ for each of the 16 models considered, together with the annual median $\bar{T}$ across all the RCMs ($\bar{T}_{50}$, i.e., the black line). Additionally, the vertical lines identify the limits of the quasi-stationary periods considered, namely the 'Control' (i.e., historical experiment), and the 'Now', 'Near', 'Mid', and 'Far' periods, (i.e., RCP-8.5). Looking at the behavior of each model, it is possible to observe an inter-model variability. The dispersion around the annual $\bar{T}_{50}$ values remains almost constant in the first three periods, while increases especially in the 'Mid' and 'Far'

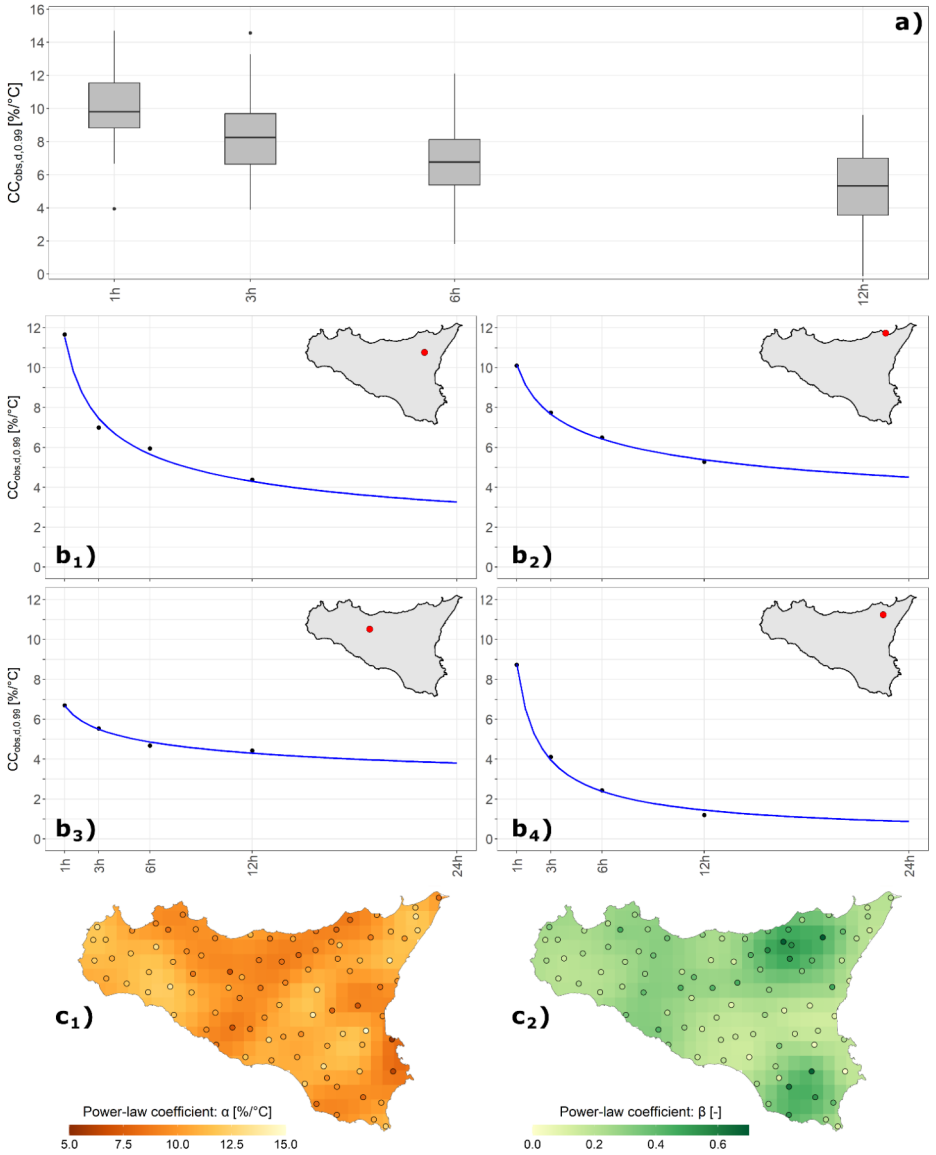

Fig. 2 Summary of results related to the time scale and spatial dependence of the $CC_{obs,d,0.99}$. Boxplots in panel **a**) depict the variability of $CC_{obs,d,0.99}$ values considering all the measurement stations for 1-, 3-, 6- and 12-hour durations. Panels **b1**) – **b4**) represent the empirical $CC_{obs,d,0.99}$ values (i.e., black dots) and power-law curves (i.e., blue lines) obtained for some measurement stations (i.e., **b1** 'Maletto', **b2** 'Patti', **b3** 'Alia', and **b4** 'Montalbano Elicona'). Spatial distribution of the power-law parameters α and β , obtained through Ordinary Kriging, is shown in panels **c1** and **c2**, respectively. Dots in these panels represent the at-site empirical values

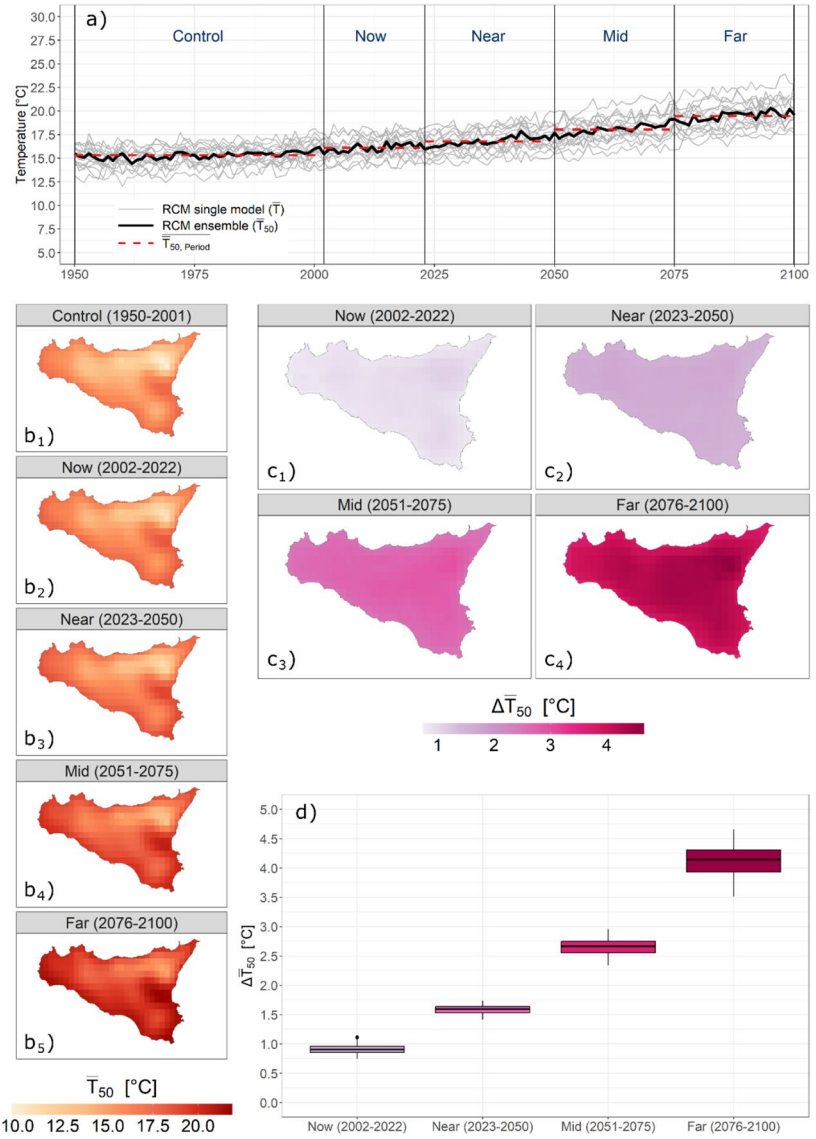

Fig. 3 Summary of results related to the future projections in temperature changes in Sicily. Panel **a**) shows the yearly temperature ($\overline{T}$) variation in Sicily from 1950–2100. Gray lines show $\overline{T}$ for 16 RCMs, while the black line represents the median $\overline{T}$ ($\overline{T}_{50}$). Vertical lines separate 'Control' (1950–2001), 'Now' (2002–2022), 'Near' (2023–2050), 'Mid' (2051–2075), and 'Far' (2076–2100) sub-periods. Red dashed lines mark the average $\overline{T}_{50}$ (*i.e.*, $\overline{T}_{50,Period}$) for each sub-period. Panels $\mathbf{b_1}$–$\mathbf{b_5}$ depict the spatial distribution of $\overline{T}_{50,Period}$, while $\mathbf{c_1}$–$\mathbf{c_4}$ show $\Delta\overline{T}_{50}$ relative to the sub-periods. Boxplots in panel **d**) summarize the variability of these changes for the whole island

sub-periods. Considering the $\overline{T}_{50}$ line, we noticed a slight increase during the 'Control' period, while there is a relevant positive trend as we move from the 'Now' to the 'Far' period. This emphasizes the need of adopting quasi-stationary periods rather than a single future period (e.g., 2023–2100) to avoid significant underestimation of the $\Delta\overline{T}_{50}$ values, especially in the last part of the century. Finally, the dashed red lines represent the average $\overline{T}_{50}$ in each period (i.e., $\overline{\overline{T}_{50,Period}}$). For the entire island, we pass from a value of ~15.5 °C during the 'Control' period, to a value of ~19.5 °C at the end of the 21st century, namely a + 4 °C variation in the mean annual temperature. Regardless of the main topic of this work, reaching this value might exacerbate droughts, water scarcity and desertification in this area (Carvalho et al. 2022; Noto et al. 2023a, b), resulting in a concrete risk for agriculture and biodiversity (Iglesias et al. 2011; Das et al. 2023).

Before proceeding further with the analysis, it is essential to address a key issue in the use of climate model results, namely the potential presence of systematic biases. These are already evident when considering the variability of $\overline{T}$ for each RCM in Fig. 3-a. In Figure S.4, we compared the empirical cumulative density function (ECDF) of $\overline{T}_{50}$ in the 'Control' period with the one derived from the observed temperatures collected from the AdB network for the period 1960–2005 (i.e., the period that offers the greatest data density and consistency). Following the same methodology applied to RCM outputs, daily temperature values were first annually averaged for each station. Then, for each year, the median value was calculated considering all the available stations. The comparison of the curves shows a negative bias in the ensemble. However, the two ECDFs have a similar shape, indicating no change in the tails of the distribution, but rather a uniform shift. Since the adopted methodology focuses on temperature changes (i.e., $\Delta\overline{T}_{50}$) rather than absolute values, it is possible to bypass the application of bias correction techniques to the RCM ensemble. Indeed, assuming that the systematic bias remains consistent in the future scenario, we can effectively neglect it when Eq. 6 is applied.

The spatial variability of $\overline{\overline{T}_{50,Period}}$ in Sicily is shown in Fig. 3 (panels b_1 - b_5). Although the systematic bias in the RCM ensemble prevents focusing on absolute values, the orographic influence on the $\overline{\overline{T}_{50,Period}}$ spatial distribution is evident and consistent with the current climate.

Panels c_1) to c_4) in Fig. 3 illustrate the spatial distribution of $\Delta\overline{T}_{50}$ for the 'Now', 'Near', 'Mid', and 'Far' periods, respectively, compared to the 'Control' one. To quantify the variability in $\Delta\overline{T}_{50}$ across these periods, the corresponding values are presented in the boxplots in panel d). As shown, the 'Now' and 'Near' periods exhibit low variability in $\Delta\overline{T}_{50}$ values. In contrast, the variability increases markedly in the 'Mid' and peaks in the 'Far' scenario. Observing the medians in the boxplots reveals an incremental rise in temperature, which reaches approximately 0.9 °C, 1.5 °C, 2.7 °C, and 4.1 °C as we move toward the end of the century. This progression underscores the growing importance of adaptation and resilience to climate change for the future. It also stresses the urgency of implementing solid and synergistic climate policies on a global scale to effectively address these challenges (Cunha 2023). Future developments of this procedure may also consider the projected changes in relative humidity, so that the combined effects of this variable and temperature can be evaluated (Treppiedi et al. 2024).

3.3 Quasi-stationary Projections of DDF Curves

With the $CC_{obs,d,0.99}$ values for different durations (see Section 3.1) and the $\Delta \bar{T}_{50}$ for the sub-periods, it is possible to compute the adaptation factor (F_A) and obtain the projected design rainfall ($h_{fut,d,T}$) according to Eq. 2.

Figure 4-a shows the boxplots of F_A at varying durations and defined sub-periods. The blue lines connect the median value in each boxplot in each sub-period. As a direct consequence of the $CC_{obs,d,0.99}$, the median value of F_A tends to decrease sharply between 1 and 4 h, and then decreases more gradually until 24 h. Furthermore, the median values of F_A for the 'Far' period are substantially higher across all durations, because of the expected large increase in temperatures for the end of the century. Still focusing on the 'Far' period and on 1-hour duration, the median F_A reaches approximately 1.5. This suggests that, in the future, it might be necessary to increase precipitation quantile for shorter durations values by almost 50% to account for climate change impacts in Sicily. As an example, Figure S.5 shows the spatial distribution of F_A for 1- and 24-hour duration across the four periods considered. Moreover, to support practitioners and stakeholders in using our findings in hydraulic and hydrological applications, the outcomes of this study are integrated into a GIS tool (Francipane et al. 2025), which will be made available by the Sicily Region Basin Authority (Figure S.6).

By applying Eq. 2, it is possible to compute the future design rainfall, $h_{fut,d,T}$. Figure 4 shows the values of $h_{fut,d,T}$ for b) RP = 5 years and d = 1 h, c) RP = 5 years and d = 24 h, d) RP = 50 year and d = 1 h, and e) RP = 50 year and d = 24 h, across each sub-period (rows). The first row (i.e., "Reference") refers to the $h_{ref,d,T}$. Although the quantile values cannot be directly compared due to the different durations and return periods, the effects of the developed methodology are clear. In all cases, the projected design rainfall for the end of this century is expected to be higher than that derived from the RFA. This outcome is a direct consequence of rising temperatures (Masson-Delmotte et al. 2021), which will play a fundamental role in increasing the water holding capacity for the air (Lehmann et al. 2015). From the thermodynamic point of view, this favors a more pronounced increase in hourly quantiles compared to those associated with longer durations. It is also worth noting that the northeastern region of the island could be already characterized by higher design rainfall values compared to the rest of Sicily in the RFA. This pre-existing condition could further amplify the future hydrological impacts in this part of the island, which is also characterized by small catchments and is particularly prone to flash floods. Focusing on the island's main urban areas (Figure S.7), the DDFs are projected to increase by about 10 − 50% (7 − 30%) for 1-hour (24-hour) duration, depending on the sub-period considered.

4 Conclusions

Nowadays it is widely recognized that climate change is altering the characteristics of rainfall events. In the context of DDF curves and, therefore, hydraulic design and water resource management, this implies the need for frameworks that can account for the consequent presence of non-stationarity.

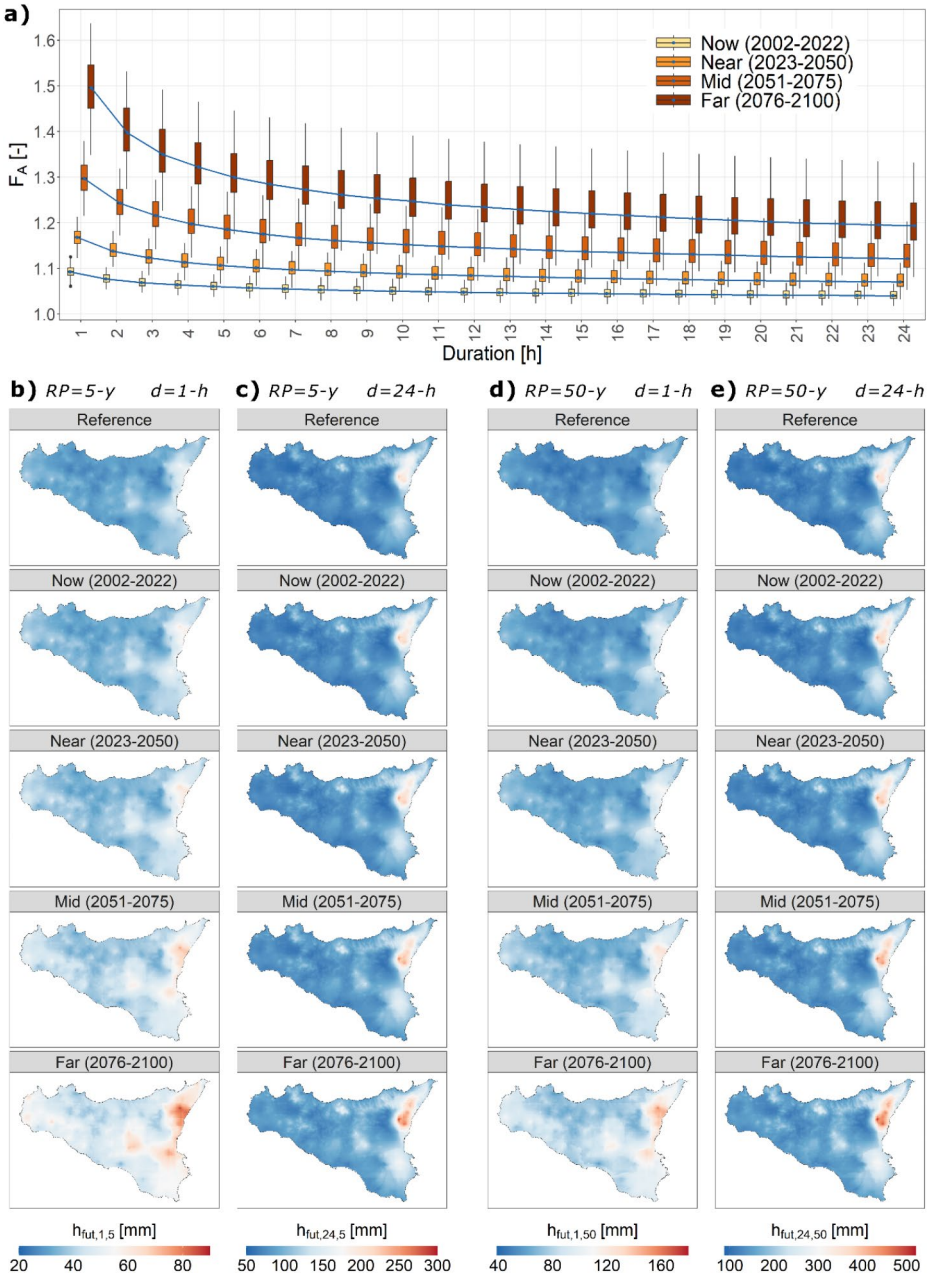

Fig. 4 Summary of results related to the quasi-stationary projections of DDF curves for Sicily. Panel **a**) show boxplots of the adaptation factor (i.e., F_A) for 1- to 24-hour durations and 'Now' (2002–2022), 'Near' (2023–2050), 'Mid' (2051–2075) and 'Far' (2076–2100) sub-periods. The blue lines connect the median value in each boxplot within the same period. Columns **b**) to **e**) represent the spatial distribution of future rainfall quantiles (i.e., $h_{fut,d,T}$) for **b**) RP = 5 years and d = 1 h, **c**) RP = 5 years and d = 24 h, **d**) RP = 50 year and d = 1 h, and **e**) RP = 50 year and d = 24 h at each time periods (rows). The first row (i.e., Reference) represent the reference quantiles ($h_{ref,d,T}$) provided by Forestieri et al. (2018)

In this study, we developed an approach based on the work of Martel et al. (2021), which involves projecting the currently existing DDFs into the future by taking into account an adaptation factor. This factor depends on the Clausius-Clapeyron scaling coefficient and changes in temperature for future quasi-stationary periods. The developed methodology was applied to the case of the Sicily region.

The presented methodology has notable strengths. On one hand, it builds on the existing DDF curves for Sicily, which are derived from a robust regionalization process and grounded in a strong statistical framework, while remaining simple and adaptable for GIS- or webGIS-based applications. At the same time, it is rooted in sound physical principles, leveraging the thermodynamics of extreme precipitation processes. Lastly, it allows for estimating design rainfall changes in a region not yet covered by CPMs, avoiding biases in GCM and RCM hourly rainfall.

On the other hand, some limitations exist, primarily related to the CC-scaling coefficient, which future studies may address more thoroughly. The approach assumes that the scaling between precipitation and temperature will remain constant in the future. This assumption could be revisited when a CPM ensemble becomes available also for Sicily. Moreover, using parametric quantile regression does not account for potential inhibition effects at higher temperatures (Yin et al. 2021). Moreover, as there is no direct correlation between the return period and the quantiles in quantile regression, the adjustment factor cannot capture the influence of the return period on extreme events.

Considering these remarks, our findings underscore the critical influence of rising temperatures on rainfall quantiles and their variability across different temporal and spatial scales. The results highlight a pronounced increase in short-duration design rainfall, that is particularly evident by the end of the 21st century, emphasizing the disproportionate sensitivity of hourly rather than daily quantiles to climate change effects. This behavior aligns with atmospheric thermodynamic principles, where shorter-duration extreme precipitation events are more directly affected by local convective processes, which are enhanced by temperature increases, the augmented capacity of the air to hold water vapor, and increased availability of precipitable water. It also aligns with results from various studies on extreme precipitation trends in Sicily. Moreover, the spatial distribution of these changes across the region confirms that some areas may be more susceptible to the increase in hourly design rainfall, which could exacerbate the risk of failure of existing hydraulic infrastructures, especially in urban environments. This may have direct implications for infrastructure planning and adaptation strategies, such as existing drainage, flood defense systems, and urban water management solutions, which may no longer be suitable to withstand such intensification of extremes. In this context, policymakers and practitioners may need to revise design standards, incorporate more flexible and adaptive infrastructure solutions, and prioritize actions in the most vulnerable areas. These insights not only highlight the importance of considering climate change impacts in planning and management of water resources and infrastructures, but also underscore the need for adaptation and resilience strategies at the regional scale (Rossi and Peres 2023).

Supplementary Information The online version contains supplementary material available at https://doi.org/10.1007/s11269-025-04162-1.

Acknowledgements The author acknowledges the support of the Basin Authority of the Hydrographic District of Sicily within the project entitled “Attività di studio e ricerca per la valutazione dell’impatto dei cambiamenti climatici e l’aggiornamento dell’idrologia di piena in attuazione della direttiva 2007/60” (Activities

of study and research for the evaluation of the climatic change impacts and the update of the flood hydrology in the implementation of guideline 2007/60) — CUP G69J17000830001.

Author Contributions DT, AF and LVN contributed to the study conception and design. Material preparation, data collection and analysis were performed by DT. The first draft of the manuscript was written by DT and DT, AF and LVN commented on previous versions of the manuscript. DT, AF and LVN read and approved the final manuscript.

Funding Open access funding provided by Università degli Studi di Palermo within the CRUI-CARE Agreement.
Not applicable.

Data Availability The SIAS dataset is available upon request on the website: http://www.sias.regione.sicilia.it/. The RFA outcomes are available upon request by contacting the authors. The RCM data are freely accessible at the following link: https://cordex.org/data-access/cordex-cmip5-data/cordex-cmip5-esgf/.

Declarations

Ethical Approval Not applicable.

Consent to Participate Not applicable.

Consent to Publish All authors consent to publish this study.

Competing Interests The authors have no relevant financial or non-financial interests to disclose. The authors declare no conflict of interest.

References

Agilan V, Umamahesh N (2016) Is the covariate based non-stationary rainfall IDF curve capable of encompassing future rainfall changes? J Hydrol 541:1441–1455

Agilan V, Umamahesh N (2017) What are the best covariates for developing non-stationary rainfall intensity-duration-frequency relationship? Adv Water Resour 101:11–22

Ali H, Fowler HJ, Lenderink G, Lewis E, Pritchard D (2021a) Consistent large-scale response of hourly extreme precipitation to temperature variation over land. Geophys Res Lett 48:e2020GL090317. https://doi.org/10.1029/2020GL090317

Ali H, Peleg N, Fowler HJ (2021b) Global scaling of rainfall with dewpoint temperature reveals considerable ocean-land difference. Geophys Res Lett 48:e2021GL093798.

Ali H, Fowler HJ, Pritchard D, Lenderink G, Blenkinsop S, Lewis E (2022) Towards quantifying the uncertainty in estimating observed scaling rates. Geophys Res Lett 49:e2022GL099138. https://doi.org/10.1029/2022GL099138

Arnone E, Pumo D, Viola F, Noto L, La Loggia G (2013) Rainfall statistics changes in Sicily. Hydrol Earth Syst Sci 17:2449–2458

Ball J, Babister M, Nathan R, Weinmann P, Weeks W, Retallick M, Testoni I (2016) Australian rainfall and runoff-a guide to flood estimation. Commonwealth of Australia

Beck HE, Zimmermann NE, Mcvicar TR, Vergopolan N, Berg A, Wood EF (2018) Present and future Köppen-Geiger climate classification maps at 1-km resolution. Sci Data 5:180214. https://doi.org/10.1038/sdata.2018.214

Brown S, Stein S, Warner J (2001) Urban drainage design manual

Carvalho D, Pereira SC, Silva R, Rocha A (2022) Aridity and desertification in the mediterranean under EURO-CORDEX future climate change scenarios. Clim Change 174:28. https://doi.org/10.1007/s10584-022-03454-4

Cheng L, Aghakouchak A (2014) Nonstationary precipitation intensity-duration-frequency curves for infrastructure design in a changing climate. Sci Rep 4:1–6

Csa (2012) Technical guide: development, interpretation and use of rainfall intensity-duration-frequency (IDF) information: Guideline for Canadian Water Resources Practitioners. Canadian Standards Association

Cunha MDC (2023) Water and environmental systems management under uncertainty: from scenario construction to robust solutions and adaptation. Water Resour Manage 37:2271–2285

Dallan E, Borga M, Fosser G, Canale A, Roghani B, Marani M, Marra F (2024) A method to assess and explain changes in sub-daily precipitation return levels from convection-permitting simulations. Water Resour Res 60:e2023WR035969.

Das S, Das J, Umamahesh N (2023) A non-stationary based approach to understand the propagation of meteorological to agricultural droughts. Water Resour Manage 37:2483–2504

Eu (2024) Common implementation strategy for the water framework directive and the flood directive - river basin management in a changing climate. In: EW DIRECTORS (ed) Guidance document

Fischer EM, Knutti R (2016) Observed heavy precipitation increase confirms theory and early models. Nat Clim Change 6:986–991

Forestieri A, Lo Conti F, Blenkinsop S, Cannarozzo M, Fowler HJ, Noto LV (2018) Regional frequency analysis of extreme rainfall in Sicily (Italy). Int J Climatol 38:e698–e716

Fowler HJ, Lenderink G, Prein AF, Westra S, Allan RP, Ban N, Barbero R, Berg P, Blenkinsop S, Do HX (2021) Anthropogenic intensification of short-duration rainfall extremes. Nat Reviews Earth Environ 2:107–122

Francipane A, Cipolla G, Treppiedi D, Noto LV (2025) Integrated hydrological modeling and analysis tool for rainfall-runoff and flow hydrograph estimation in sicilian watersheds (under revision). Environmental Modelling & Software

Giorgi F (2006) Climate change hot-spots. Geophys Res Lett 33:L08707. https://doi.org/10.1029/2006GL025734

Hardwick Jones R, Westra S, Sharma A (2010) Observed relationships between extreme sub-daily precipitation, surface temperature, and relative humidity. Geophys Res Lett 37. https://doi.org/10.1029/2010GL045081

Hengl T (2006) Finding the right pixel size. Comput Geosci 32:1283–1298

Iglesias A, Mougou R, Moneo M, Quiroga S (2011) Towards adaptation of agriculture to climate change in the mediterranean. Reg Envriron Chang 11:159–166

Iturbide M, Gutiérrez JM, Alves LM, Bedia J, Cerezo-Mota R, Cimadevilla E, Cofiño AS, Di Luca A, Faria SH, Gorodetskaya IV (2020) An update of IPCC climate reference regions for Subcontinental analysis of climate model data: definition and aggregated datasets. Earth Syst Sci Data 12:2959–2970

Jacob D, Petersen J, Eggert B, Alias A, Christensen OB, Bouwer LM, Braun A, Colette A, Déqué M, Georgievski G (2014) EURO-CORDEX: new high-resolution climate change projections for European impact research. Reg Envriron Chang 14:563–578

Koenker R, Hallock KF (2001) Quantile regression. J Economic Perspect 15:143–156

Lehmann J, Coumou D, Frieler K (2015) Increased record-breaking precipitation events under global warming. Clim Change 132:501–515

Lenderink G, Van Meijgaard E (2008) Increase in hourly precipitation extremes beyond expectations from temperature changes. Nat Geosci 1:511–514. https://doi.org/10.1038/ngeo262

Lenderink G, Van Meijgaard E (2010) Linking increases in hourly precipitation extremes to atmospheric temperature and moisture changes. Environ Res Lett 5:025208

Lenderink G, Barbero R, Loriaux J, Fowler H (2017) Super-Clausius–Clapeyron scaling of extreme hourly convective precipitation and its relation to large-scale atmospheric conditions. J Clim 30:6037–6052

Llasat MC, Moral D, Cortès A, M., Rigo T (2021) Convective precipitation trends in the Spanish mediterranean region. Atmos Res 257:105581

Magnus G (1844) Versuche über die spannkräfte des wasserdampfs. Ann Phys 137:225–247

Martel J-L, Brissette FP, Lucas-Picher P, Troin M, Arsenault R (2021) Climate change and rainfall intensity–duration–frequency curves: overview of science and guidelines for adaptation. J Hydrol Eng 26:03121001

Masson-Delmotte V, Zhai P, Pirani A, Connors SL, Péan C, Berger S, Caud N, Chen Y, Goldfarb L, Gomis M (2021) Climate change 2021: the physical science basis. Contribution Working Group I Sixth Assess Rep Intergovernmental Panel Clim Change 2:2391

Mazoyer M, Roehrig R, Duffourg F, Nuissier O (2023) Simulating a mediterranean heavy-precipitating event with parametrized convection: role of subgrid-scale topography. Q J R Meteorol Soc 149:1–18. https://doi.org/10.1002/qj.4369

Milly PC, Betancourt J, Falkenmark M, Hirsch RM, Kundzewicz ZW, Lettenmaier DP, Stouffer RJ (2008) Stationarity is dead: whither water management? Science 319:573–574

Mondal A, Mujumdar PP (2015) Modeling non-stationarity in intensity, duration and frequency of extreme rainfall over India. J Hydrol 521:217–231. https://doi.org/10.1016/j.jhydrol.2014.11.071

Moradian S, Torabi Haghighi A, Asadi M, Mirbagheri SA (2023) Future changes in precipitation over Northern Europe based on a multi-model ensemble from CMIP6: focus on Tana river basin. Water Resour Manage 37:2447–2463

Noor M, Ismail T, Shahid S, Asaduzzaman M, Dewan A (2022) Projection of rainfall intensity-duration-frequency curves at ungauged location under climate change scenarios. Sustainable Cities Soc 83:103951

Noto L, Cipolla G, Pumo D, Francipane A (2023a) Climate change in the mediterranean basin (Part II): a review of challenges and uncertainties in climate change modeling and impact analyses. Water Resour Manage 37:2307–2323

Noto LV, Cipolla G, Francipane A, Pumo D (2023b) Climate change in the mediterranean basin (part I): induced alterations on climate forcings and hydrological processes. Water Resour Manage 37:2287–2305

O'gorman PA (2015) Precipitation extremes under climate change. Curr Clim Change Rep 1:49–59

Ouarda TB, Yousef LA, Charron C (2019) Non-stationary Intensity-Duration-Frequency curves integrating information concerning teleconnections and climate change. Int J Climatol 39:2306–2323

Panthou G, Mailhot A, Laurence E, Talbot G (2014) Relationship between surface temperature and extreme rainfalls: A Multi-Time-Scale and Event-Based analysis**. J Hydrometeorol 15:1999–2011. https://doi.org/10.1175/JHM-D-14-0020.1

Pfahl S, O'gorman PA, Fischer EM (2017) Understanding the regional pattern of projected future changes in extreme precipitation. Nat Clim Change 7:423–427

Purr C, Brisson E, Ahrens B (2021) Convective rain cell characteristics and scaling in climate projections for Germany. Int J Climatol 41:3174–3185

Raffa M, Adinolfi M, Reder A, Marras GF, Mancini M, Scipione G, Santini M, Mercogliano P (2023) Very high resolution projections over Italy under different CMIP5 IPCC scenarios. Sci Data 10:238

Rossi G, Peres DJ (2023) Climatic and other global changes as current challenges in improving water systems management: lessons from the case of Italy. Water Resour Manage 37:2387–2402

Salas J, Obeysekera J, Vogel R (2018) Techniques for assessing water infrastructure for nonstationary extreme events: A review. Hydrol Sci J 63:325–352

Sarhadi A, Soulis ED (2017) Time-varying extreme rainfall intensity-duration-frequency curves in a changing climate. Geophys Res Lett 44:2454–2463

Schlef KE, Kunkel KE, Brown C, Demissie Y, Lettenmaier DP, Wagner A, Wigmosta MS, Karl TR, Easterling DR, Wang KJ (2023) Incorporating non-stationarity from climate change into rainfall frequency and intensity-duration-frequency (IDF) curves. J Hydrol 616:128757

Schulzweida U, Kornblueh L, Quast R (2019) CDO user guide.

Schwalm CR, Glendon S, Duffy PB (2020) RCP8. 5 tracks cumulative CO2 emissions. Proc Natl Acad Sci 117:19656–19657

Shehu B, Willems W, Stockel H, Thiele L-B, Haberlandt U (2023) Regionalisation of rainfall depth–duration–frequency curves with different data types in Germany. Hydrol Earth Syst Sci 27:1109–1132

Sottile G, Francipane A, Adelfio G, Noto LV (2022) A PCA-based clustering algorithm for the identification of stratiform and convective precipitation at the event scale: an application to the sub-hourly precipitation of Sicily, Italy. Stoch Env Res Risk Assess 36:2303–2317

Treppiedi D, Cipolla G, Francipane A, Noto L (2021) Detecting precipitation trend using a multiscale approach based on quantile regression over a mediterranean area. Int J Climatol 41:5938–5955

Treppiedi D, Cipolla G, Francipane A, Cannarozzo M, Noto LV (2023a) Investigating the reliability of stationary design rainfall in a mediterranean region under a changing climate. Water 15:2245

Treppiedi D, Cipolla G, Noto LV (2023b) Convective precipitation over a mediterranean area: from identification to trend analysis starting from high-resolution rain gauges data. Int J Climatol 43:293–313

Treppiedi D, Villarini G, Noto LV (2024) Climate change exacerbates the compounding of heat stress and flooding in the mid-latitudes. Int J Climatol 44:2283–2296. https://doi.org/10.1002/joc.8453

Treppiedi D, Villarini G, Bender J, Noto LV (2025) Precipitation extremes projected to increase and to occur in different times of the year. Environ Res Lett 20:014014. https://doi.org/10.1088/1748-9326/ad984f

Tsakiris G, Loucks D (2023) Adaptive water resources management under climate change: an introduction. Water Resour Manage 37:2221–2233

Wasko C, Sharma A (2015) Steeper Temporal distribution of rain intensity at higher temperatures within Australian storms. Nat Geosci 8:527–529. https://doi.org/10.1038/ngeo2456

Wasko C, Sharma A, Johnson F (2015) Does storm duration modulate the extreme precipitation-temperature scaling relationship? Geophys Res Lett 42:8783–8790. https://doi.org/10.1002/2015GL066274

Yan L, Xiong L, Jiang C, Zhang M, Wang D, Xu CY (2021) Updating intensity–duration–frequency curves for urban infrastructure design under a changing environment. Wiley Interdisciplinary Reviews: Water 8:e1519

Yin J, Guo S, Gentine P, Sullivan SC, Gu L, He S, Chen J, Liu P (2021) Does the hook structure constrain future flood intensification under anthropogenic climate warming? Water Resour Res 57:e2020WR028491.

Zhao W, Kinouchi T, Nguyen HQ (2021) A framework for projecting future intensity-duration-frequency (IDF) curves based on CORDEX Southeast Asia multi-model simulations: an application for two cities in Southern Vietnam. J Hydrol 598:126461

Zittis G, Almazroui M, Alpert P, Ciais P, Cramer W, Dahdal Y, Fnais M, Francis D, Hadjinicolaou P, Howari F (2022) Climate change and weather extremes in the Eastern Mediterranean and Middle East. Rev Geophys 60:e2021RG000762.